Space-time hexahedral finite element methods for parabolic evolution problems

Ulrich Langer   Andreas Schafelner

A–4040 LINZ, ALTENBERGERSTRASSE 69, AUSTRIA

Space-time hexahedral finite element methods for parabolic evolution problems[*]

Ulrich Langer[1] and Andreas Schafelner[2]

[1]*Institute for Computational Mathematics*
Johannes Kepler University Linz
Altenberger Str. 69, 4040 Linz, Austria
[2]*Doctoral Program "Computational Mathematics"*
Johannes Kepler University Linz
Altenberger Str. 69, A-4040 Linz, Austria

Abstract

We present locally stabilized, conforming space-time finite element methods for parabolic evolution equations on hexahedral decompositions of the space-time cylinder. Tensor-product decompositions allow for anisotropic a priori error estimates, that are explicit in spatial and temporal meshsizes. Moreover, tensor-product finite elements are suitable for anisotropic adaptive mesh refinement strategies provided that an appropriate a posteriori discretization error estimator is available. We present such anisotropic adaptive strategies together with numerical experiments.

Keywords: Parabolic initial-boundary value problems, Space-time finite element methods, Hexahedral meshes, Anisotropic a priori error estimates, Anisotropic adaptivity

1 Introduction

We consider the parabolic initial-boundary value problem (IBVP), find u such that

$$\partial_t u - \mathrm{div}_x(\nu \, \nabla_x u) = f \text{ in } Q, \ u = u_D := 0 \text{ on } \Sigma, \ u = u_0 := 0 \text{ on } \Sigma_0, \qquad (1)$$

as a model problem typically arising in heat conduction and diffusion, where $Q = \Omega \times (0, T)$, $\Sigma = \partial\Omega \times (0, T)$, and $\Sigma_0 = \Omega \times \{0\}$. The spatial domain $\Omega \subset \mathbb{R}^d$, $d = 1, 2, 3$, is assumed to be bounded and Lipschitz, $T > 0$ is the terminal time, $f \in L_2(Q)$ denotes a given source, and $\nu \in L_\infty(Q)$ is a given uniformly bounded and positive coefficient that may discontinuously depend on the spatial variable $x = (x_1, \ldots, x_d)$ and the time variable t, but $\nu(x, t)$ should be of bounded variation in t for almost all $x \in \Omega$. Then there is a unique weak solution $u \in V_0 := \{v \in L_2(0, T; H_0^1(\Omega)) : \partial_t u \in L_2(0, T; H^{-1}(\Omega)), v = 0 \text{ on } \Sigma_0\}$ of the IBVP (1); see, e.g.,

[4, 13]. Moreover, $\partial_t u$ and $Lu := -\text{div}_x(\nu \nabla_x u)$ belong to $L_2(Q)$; see [3]. The latter property is called maximal parabolic regularity. In this case, the parabolic partial differential equation $\partial_t u - \text{div}_x(\nu \nabla_x u) = f$ holds in $L_2(Q)$. This remains even valid for inhomogeneous initial conditions $u_0 \in H_0^1(\Omega)$.

Time-stepping methods in combination with some spatial discretization method like the finite element method (FEM) are still the standard approach to the numerical solution of IBVP like (1); see, e.g., [15]. This time-stepping approach as well as the more recent discontinuous Galerkin, or discontinuous Petrov-Galerkin methods based on time slices or slabs are in principle sequential. The sequential nature of these methods hampers the full space-time adaptivity and parallelization; but see the overview paper [5] for parallel-in-time methods. Space-time finite element methods on fully unstructured decomposition of the space-time cylinder Q avoid these bottlenecks; see [14] for an overview of such kind of space-time methods.

In this paper, we follow our preceding papers [8, 10, 9], and construct locally stabilized, conforming space-time finite element schemes for solving the IBVP (1), but on hexahedral meshes that are more suited for anisotropic refinement than simplicial meshes used in [8, 10, 9]. We mention that SUPG/SD and Galerkin/least-squares stabilizations of time-slice finite element schemes for solving transient problems were already used in early papers; see, e.g., [7] and [6]. Section 2 recalls the construction of locally stabilized space-time finite element schemes, the properties of the corresponding discrete bilinear form, and the a priori discretization error estimates from [8, 10, 9]. In Section 3, we derive new anisotropic a priori discretization estimates for hexahedral tensor-product meshes, and we provide anisotropic adaptive mesh refinement strategies that are based on a posteriori error estimates, anisotropy indicators, and anisotropic adaptive mesh refinement using hanging nodes. In Section 4, we present and discuss numerical results for an example where a singularity occurs in the spatial gradient of the solution. The large-scale system of space-time finite element equations is always solved by means of the Flexible Generalized Minimal Residual (FGMRES) method preconditioned by space-time algebraic multigrid.

2 Space-time finite element methods

In this section, we will briefly describe the space-time finite element method based on localized time-upwind stabilizations; for details of the construction and analysis, we refer to our previous work [8, 10, 9]. Let $\mathcal{T}_h$ be a shape regular decomposition of the space-time cylinder Q, i.e., $\overline{Q} = \bigcup_{K \in \mathcal{T}_h} \overline{K}$, and $K \cap K' = \emptyset$ for all K and K' from $\mathcal{T}_h$ with $K \neq K'$; see, e.g., [2] for more details. Furthermore, we assume that ν is piecewise smooth, and possible discontinuities are aligned with the triangulation as usual. On the basis of the triangulation $\mathcal{T}_h$, we define the space-time finite element space

$$V_{0h} = \{v \in C(\overline{Q}) : v(x_K(\cdot)) \in \mathbb{P}_p(\hat{K}), \, \forall K \in \mathcal{T}_h, \, v = 0 \text{ on } \overline{\Sigma} \cap \overline{\Sigma}_0\},$$

where $x_K(\cdot)$ denotes the map from the reference element $\hat{K}$ to the finite element $K \in \mathcal{T}_h$, and $\mathbb{P}_p(\hat{K})$ is the space of polynomials of the degree p on the reference element $\hat{K}$. Since we are in the maximal parabolic regularity setting, the parabolic Partial Differential Equation (PDE) is valid in $L_2(Q)$. Multiplying the PDE (1), restricted to $K \in \mathcal{T}_h$, by a locally scaled upwind test function $v_{h,K}(x,t) := v_h(x,t) + \theta_K h_K \partial_t v_h(x,t)$, $v_h \in V_{0h}$, integrating over K, summing over all elements, applying

integration by parts, and incorporating the Dirichlet boundary conditions, we obtain the variational consistency identity

$$a_h(u, v_h) = \ell_h(v_h), \quad \forall v_h \in V_{0h}, \tag{2}$$

with the mesh-dependent bilinear form

$$a_h(u, v_h) = \sum_{K \in \mathcal{T}_h} \int_K \left[\partial_t u v_h + \theta_K h_K \partial_t u \partial_t v_h \right. \tag{3}$$
$$\left. + \nu \nabla_x u \cdot \nabla_x v_h - \theta_K h_K \mathrm{div}_x(\nu \nabla_x u) \partial_t v_h \right] \mathrm{d}K,$$

and the mesh-dependent linear form

$$\ell_h(v_h) = \sum_{K \in \mathcal{T}_h} \int_K \left[f v_h + \theta_K h_K f \partial_t v_h \right] \mathrm{d}K.$$

Now we apply the Galerkin principle, i.e., we look for a finite element approximation $u_h \in V_{0h}$ to u such that

$$a_h(u_h, v_h) = l_h(v_h), \quad \forall v_h \in V_{0h}. \tag{4}$$

Using Galerkin orthogonality (subtracting (4) from (2)), and coercivity and extended boundedness of the bilinear form (3), we can show the following Céa-like best approximation estimate; see [8, 10, 9] for the proofs.

Theorem 1. *Let* $u \in H_0^{L,1}(Q) := \{v \in V_0 \cap H^1(Q) : Lv := -\mathrm{div}_x(\nu \nabla_x v) \in L_2(Q)\}$ *and* $u_h \in V_{0h}$ *be the solutions of the parabolic IBVP (1) and the space-time finite element scheme (4), respectively. Then the discretization error estimate*

$$\|u - u_h\|_h \leq \inf_{v_h \in V_{0h}} \left(\|u - v_h\|_h + \frac{\mu_b}{\mu_c} \|u - v_h\|_{h,*} \right) \tag{5}$$

is valid provided that $\theta_K = O(h_K)$ *is sufficiently small, where*

$$\|v\|_h^2 = \frac{1}{2} \|v\|_{L_2(\Sigma_T)}^2 + \sum_{K \in \mathcal{T}_h} \left[\theta_K h_K \|\partial_t v\|_{L_2(K)}^2 + \|\nu^{1/2} \nabla_x v\|_{L_2(K)}^2 \right],$$

$$\|v\|_{h,*}^2 = \|v\|_h^2 + \sum_{K \in \mathcal{T}_h} \left[(\theta_K h_K)^{-1} \|v\|_{L_2(K)}^2 + \theta_K h_K \|\mathrm{div}_x(\nu \nabla_x v)\|_{L_2(K)}^2 \right].$$

The best-approximation error estimate (5) now leads to convergence rate estimates under additional regularity assumptions. If the solution u of (1) belongs to $H_0^{L,1}(Q) \cap H^l(Q)$, $l > 1$, then $\|u - u_h\|_h \leq c(u) h^{s-1}$, where $s = \min\{l, p + 1\}$, $h = \min_{K \in \mathcal{T}_h} h_K$, $c(u)$ depends on the regularity of u. We refer the reader to [8, Theorem 13.3] and [10, Theorem 3] for the proof of more detailed estimates in terms of the local mesh-sizes h_k and the local regularity of the solution u.

3 Anisotropic a priori and a posteriori error estimates

The convergence rate estimates presented at the end of the previous section consider only isotropic finite elements, but in many application the solution u evolves differently with respect to time and space directions. So, we should permit anisotropic

finite elements with different mesh sizes in different directions. This raises the question whether we can obtain (localized) a priori estimates that are explicit in spatial and temporal mesh sizes as well as in spatial and temporal regularity assumptions imposed on the solution u. We refer to [1] for a comprehensive summary of anisotropic finite elements. For the remainder of this section, we will now assume that K is a *brick element* (hexahedral element for the case $d = 2$), i.e., the edges of K are parallel to the coordinate axes. Moreover, we assume that $u \in H^l(Q)$ with $l > (d+1)/2$ an integer such that we can use the Lagrange interpolation operator I_h. Let $h_{K,i} = \max\{|x_i - x'_i| : x, x' \in K\}$, then $h_{K,x} = \max_{i=1,\ldots,d} h_{K,i}$ and $h_{K,t} = h_{K,d+1}$. Furthermore, let $e_h = u - I_h u$ and $s = \min\{l, p+1\}$, where p is the polynomial degree of the finite element shape functions in every coordinate direction. Using the anisotropic interpolation error estimates from [1], we get

$$\|e_h\|^2_{L_2(K)} \le c \left(\sum_{j=1}^d h_{K,j}^{2s} \|\partial_{x_j}^s u\|^2_{L_2(K)} + h_{K,t}^{2s} \|\partial_t^s u\|^2_{L_2(K)} \right),$$

$$\|\partial_t(e_h)\|^2_{L_2(K)} \le c \left(\sum_{j=1}^d h_{K,j}^{2(s-1)} \|\partial_t \partial_{x_j}^{(s-1)} u\|^2_{L_2(K)} + h_{K,t}^{2(s-1)} \|\partial_t^s u\|^2_{L_2(K)} \right),$$

$$\|\partial_{x_i}(e_h)\|^2_{L_2(K)} \le c \left(\sum_{j=1}^d h_{K,j}^{2(s-1)} \|\partial_{x_i} \partial_{x_j}^{(s-1)} u\|^2_{L_2(K)} + h_{K,t}^{2(s-1)} \|\partial_{x_i} \partial_t^{(s-1)} u\|^2_{L_2(K)} \right),$$

$$\|\partial_{x_i}^2(e_h)\|^2_{L_2(K)} \le c \left(\sum_{j=1}^d h_{K,j}^{2(s-2)} \|\partial_{x_i}^2 \partial_{x_j}^{(s-2)} u\|^2_{L_2(K)} + h_{K,t}^{2(s-2)} \|\partial_{x_i}^2 \partial_t^{(s-2)} u\|^2_{L_2(K)} \right),$$

for $i = 1, \ldots, d$, where c denotes generic positive constants. These estimates of the interpolation error and its derivatives immediately lead to the corresponding interpolation error estimates with respect to the norms $\|\cdot\|_h$ and $\|\cdot\|_{h,*}$.

Lemma 1. *Let $u \in H_0^{L,1}(Q) \cap H^l(Q)$, $l \in \mathbb{N}$ with $l > (d+1)/2$, and let $\mathcal{T}_h$ be a decomposition of Q into brick elements. Then the anisotropic interpolation error estimates*

$$\|u - I_h u\|_h \le \left(\sum_{K \in \mathcal{T}_h} h_{K,x}^{2(s-1)} \mathfrak{c}_1(u, K) + h_{K,t}^{2(s-1)} \mathfrak{c}_2(u, K) \right)^{1/2}, \tag{6}$$

$$\|u - I_h u\|_{h,*} \le \left(\sum_{K \in \mathcal{T}_h} h_{K,x}^{2(s-1)} \mathfrak{c}_{1,*}(u, K) + h_{K,t}^{2(s-1)} \mathfrak{c}_{2,*}(u, K) \right)^{1/2} \tag{7}$$

hold, where $s = \min\{l, p+1\}$, and $\mathfrak{c}_1(u, K)$, $\mathfrak{c}_2(u, K)$, $\mathfrak{c}_{1,*}(u, K)$ and $\mathfrak{c}_{2,*}(u, K)$ can easily be computed from the interpolation error estimates given above.

Combining the interpolation error estimates (6) and (7) with the best approximation estimate (5), we can immediately derive an a priori discretization error estimate.

Theorem 2. *Let the assumptions of Theorem 1 (best approximation estimate) and of Lemma 1 (anisotropic interpolation error estimates) be fulfilled. Then the*

anisotropic a priori discretization error estimate

$$\|u - u_h\|_h \leq \left(\sum_{K \in \mathcal{T}_h} h_{K,x}^{2(s-1)} \mathfrak{C}_1(u, K) + h_{K,t}^{2(s-1)} \mathfrak{C}_2(u, K) \right)^{1/2},$$

is valid, where $s = \min\{l, p+1\}$, and $\mathfrak{C}_1(u, K)$ and $\mathfrak{C}_2(u, K)$ can be computed from (6) *and* (7).

In the computational practice, we would like to replace the uniform mesh refinement by adaptive space-time mesh refinement that takes care of possible anisotropic features of the solution in space and time. Here brick finite elements with hanging nodes, as implemented in MFEM (see next section), are especially suited. To drive anisotropic adaptive mesh refinement, we need a localizable a posteriori error estimator providing local error indicators, and an anisotropy indicator defining the refinement directions in each brick element $K \in \mathcal{T}_h$.

We use the functional a posteriori error estimators introduced by Repin; see his monograph [12]. Repin proposed two error majorants $\mathfrak{M}_1$ and $\mathfrak{M}_2$ from which the local error indicators

$$\eta_{1,K}^2(u_h) = \frac{1}{\delta} \int_K \left[(1 + \beta)|\mathbf{y} - \nu \nabla_x u_h|^2 + \frac{1 + \beta}{\beta} c_{F\Omega}^2 |f - \partial_t u_h + \text{div}_x \mathbf{y}|^2 \right] dK \text{ and}$$

$$\eta_{2,K}^2(u_h) = \frac{1}{\delta} \int_K (1 + \beta) \left[|\mathbf{y} - \nu \nabla_x u_h + \nabla_x \vartheta|^2 + \frac{c_{F\Omega}^2 (1 + \beta)}{\beta} |f - \partial_t u_h - \partial_t \vartheta + \text{div}_x \mathbf{y}|^2 \right] dK$$

$$+ \gamma \|\vartheta(\cdot, T)\|_\Omega^2 + 2 \int_K \left[\nabla_x u_h \cdot \nabla_x \vartheta + (\partial_t u_h - f)\vartheta \right] dK$$

can be derived for each element $K \in \mathcal{T}_h$, where $\mathbf{y} \in H(\text{div}_x, Q)$ is an arbitrary approximation to the flux, $\vartheta \in H^1(Q)$ is also an arbitrary function, $\delta \in (0, 2]$, $\beta > \mu$, $\mu \in (0, 1)$, and $\gamma > 1$. The positive constant $c_{F\Omega}$ denotes the constant in the inequality $\|v\|_{L_2(Q)} \leq c_{F\Omega} \|\sqrt{\nu} \nabla_x v\|_{L_2(Q)}$ for all $v \in L_2(0, T; H_0^1(\Omega))$, which is nothing but the Friedrichs constant for the spatial domain Ω in the case $\nu = 1$. Both majorants provide a guaranteed upper bound for the errors

$$\|u - u_h\|_{(1, 2-\delta)}^2 \leq \sum_{K \in \mathcal{T}_h} \eta_{1,K}^2(u_h) \quad \text{and} \quad \|u - u_h\|_{(1 - \frac{1}{\gamma}, 2-\delta)}^2 \leq \sum_{K \in \mathcal{T}_h} \eta_{2,K}^2(u_h),$$

where $\|v\|_{(\epsilon, \kappa)}^2 := \kappa \|\sqrt{\nu} \nabla_x v\|_Q^2 + \epsilon \|v\|_{\Sigma_T}^2$. Once we have computed the local error indicators $\eta_K(u_h)$ for all elements $K \in \mathcal{T}_h$, we use *Dörfler marking* to determine a set $\mathcal{M} \subseteq \mathcal{T}_h$ of elements that will be marked for refinement. The set $\mathcal{M}$ is of (almost) minimal cardinality such that

$$\sigma \sum_{K \in \mathcal{T}_h} \eta_K(u_h)^2 \leq \sum_{K \in \mathcal{M}} \eta_K(u_h)^2,$$

where $\sigma \in (0, 1)$ is a bulk parameter. Let $\mathbf{E}_K \in \mathbb{R}^{d+1}$ with entries $E_i^{(K)}$, $i = 1, \ldots, d+1$, and $\chi \in (0, 1)$. In order to determine how to subdivide a marked element, we use the following heuristics: for each $K \in \mathcal{M}$, subdivide K in direction x_i iff $E_i^{(K)} > \chi |\mathbf{E}_K|$. In particular, we choose

$$\left(E_i^{(K)} \right)^2 := \begin{cases} \int_K (y_i - \nu \partial_{x_i} u_h)^2 \, dK, & i \leq d, \\ \int_K (\mathbf{d_t}_h - \partial_t u_h)^2 \, dK, & i = d+1, \end{cases}$$

5

as our local anisotropy vector $\mathbf{E}_K$, where $\mathbf{y}_h = (y_i)_{i=1}^d$, $\mathbf{d}_{\mathbf{t}h} = R_h(\partial_t u_h)$, and R_h is some nodal averaging operator like in a Zienkiewicz-Zhu approach.

4 Numerical Results

Now let $\{p^{(j)} : j = 1, \ldots, N_h\}$ be the finite element nodal basis of V_{0h}, i.e., $V_{0h} = \mathrm{span}\{p^{(1)}, \ldots, p^{(N_h)}\}$, where N_h is the number of all space-time unknowns (dofs). Then we can express the approximate solution u_h in terms of this basis, i.e., $u_h(x,t) = \sum_{j=1}^{N_h} u_j\, p^{(j)}(x,t)$. Inserting this representation into (4), and testing with $p^{(i)}$, we get the linear system $K_h \underline{u}_h = \underline{f}_h$ for determining the unknown coefficient vector $\underline{u}_h = (u_j)_{j=1,\ldots,N_h} \in \mathbb{R}^{N_h}$, where $K_h = (a_h(p^{(j)}, p^{(i)}))_{i,j=1,\ldots,N_h}$ and $\underline{f}_h = (\ell_h(p^{(i)}))_{i=1,\ldots,N_h}$. The system matrix K_h is non-symmetric, but positive definite due to coercivity of the bilinear form $a_h(\cdot,\cdot)$. Thus, in order to obtain a numerical solution to the to the IBVP (1), we just need to solve one linear system of algebraic equations. This is always solved by means of the FGMRES method preconditioned by space-time algebraic multigrid (AMG). We use the finite element library MFEM [11] to implement our space-time finite element solver. The AMG preconditioner is realized via *BoomerAMG*, provided by the linear solver library *hypre*[1]. We start the linear solver with initial guess $\mathbf{0}$, and stop once the initial residual has been reduced by a factor of 10^{-8}. In order to accelerate the solver in case of adaptive refinements, we also employ *Nested Iterations.* Here, we interpolate the finite element approximation from the previous mesh to the current mesh, and use that as an initial guess for FGMRES. Moreover, we stop the linear solver earlier, e.g. once the residual is reduced by a factor of 10^{-2}. Furthermore, we will use the notation $\mathcal{O}(h^\alpha) = \mathcal{O}(N_h^{-\alpha/(d+1)})$ to indicate the corresponding convergence rates.

Let $Q = \Omega \times (0,1)$, where $\Omega = (0,1)^2 \setminus \{(x_1, 0) \in \mathbb{R}^2 : 0 \leq x_1 < 1\}$ is a "slit domain" that is not Lipschitz. Moreover, we choose the constant diffusion coefficient $\nu \equiv 1$, and the manufactured solution $u(r,\phi,t) = t\, r^\alpha \sin(\alpha\phi)$, where (r,ϕ) are polar coordinates with respect to (x_1, x_2), and $\alpha = 0.5$. We know[2] that u only belongs to $H^{1+\alpha}(Q)$ due to the singularity of the gradient at $(0,0)$. Hence, uniform mesh refinement will result in a reduced convergence rate of $\mathcal{O}(h^\alpha)$.

In order to properly realize the adaptive refinement strategies, we need to choose appropriate $\mathbf{y}$ and ϑ. For the first majorant, we reconstruct an improved flux $\mathbf{y}_h^{(0)} = R_h(\nabla_x u_h)$, where R_h is a nodal averaging operator. We then improve this flux by applying a few CG steps to the minimization problem $\min_{\mathbf{y}} \mathfrak{M}_1$, obtaining the final flux $\mathbf{y}_h^{(1)}$ that is then used in the estimator. For the second majorant, we follow the same procedure, but right before postprocssing the flux, we first apply some CG iteration to another minimization problem $\min_\vartheta \mathfrak{M}_2$.

For linear finite elements, we observe at least optimal convergence rates for both error estimators. Anisotropic refinements, with the anisotropy parameter $\chi = 0.1$, manage to obtain a better constant than isotropic refinements; see Fig. 1 (upper left). For quadratic finite elements, anisotropic adaptive refinements, with $\chi = 0.15$, manage to recover the optimal rate of $\mathcal{O}(h^2)$, while isotropic adaptive refinements result in a reduced rate of $\mathcal{O}(h^{1.25})$; see Fig. 1 (upper right). The efficiency indices

---

[1] https://github.com/hypre-space/hypre
[2] https://math.nist.gov/amr-benchmark/index.html

are rather stable for isotropic refinements, while some oscillations can be observed for anisotropic refinements; see Fig. 1 (lower right).
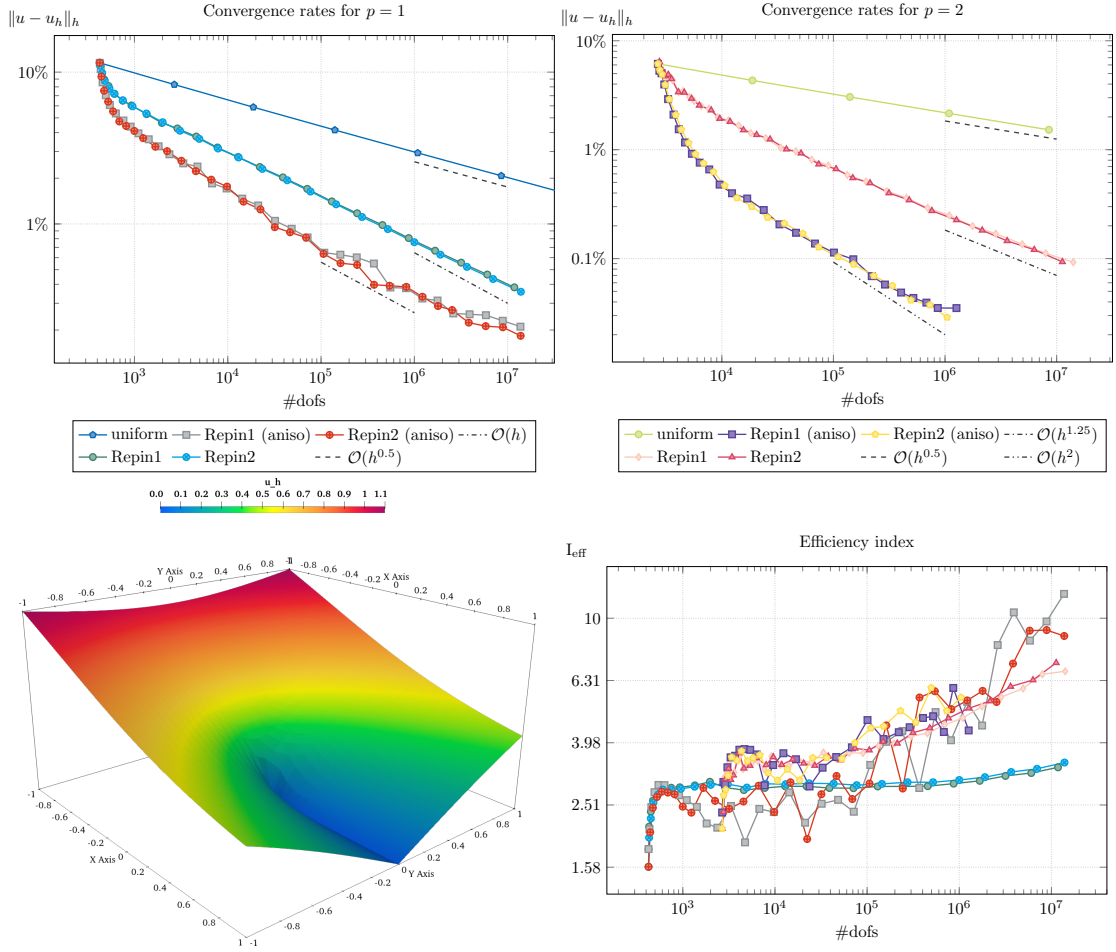

Fig. 1: Convergence rates for $p = 1$ (upper left); convergence rates for $p = 2$ (upper right); plot of $u(\cdot, \cdot, 1)$ (lower left); efficiency indices for $p = 1, 2$, with the respective colors from the upper plots (lower right).

References

[1] APEL, T. *Anisotropic finite elements: Local estimates and applications.* Teubner, Stuttgart, 1999.

[2] CIARLET, P. G. *The Finite Element Method for Elliptic Problems.* North-Holland Publishing Co., Amsterdam-New York-Oxford, 1978.

[3] DIER, D. Non-autonomous maximal regularity for forms of bounded variation. *J. Math. Anal. Appl. 425* (2015), 33–54.

[4] EVANS, L. *Partial Differential Equations*, vol. 19 of *Graduate Studies in Mathematics*. American Mathematical Society, 2010.

[5] GANDER, M. J. 50 years of time parallel integration. In *Multiple Shooting and Time Domain Decomposition*. Springer Verlag, Heidelberg, Berlin, 2015, pp. 69–114.

[6] HUGHES, T., FRANCA, L., AND HULBERT, G. A new finite element formulation for computational fluid dynamics: VIII. The Galerkin/least-squares method for advection-diffusive equations. *Comput. Methods Appl. Mech. Engrg.* *73* (1989), 173–189.

[7] JOHNSON, C., AND SARANEN, J. Streamline diffusion methods for the incompressible Euler and Navier-Stokes equations. *Math. Comp. 47*, 175 (1986), 1–18.

[8] LANGER, U., NEUMÜLLER, M., AND SCHAFELNER, A. Space-time Finite Element Methods for Parabolic Evolution Problems with Variable Coefficients. In *Advanced Finite Element Methods with Applications*, T. Apel, U. Langer, A. Meyer, and O. Steinbach, Eds., vol. 128 of *LNCSE*. Springer, Berlin, Heidelberg, New York, 2019, ch. 13, pp. 247–275.

[9] LANGER, U., AND SCHAFELNER, A. Adaptive Space-Time Finite Element Methods for Non-autonomous Parabolic Problems with Distributional Sources. *Comput. Methods Appl. Math. 20*, 4 (2020), 677–693.

[10] LANGER, U., AND SCHAFELNER, A. Space-Time Finite Element Methods for Parabolic Initial-Boundary Value Problems with Non-smooth Solutions. In *Large-Scale Scientific Computing. LSSC 2019*, I. Lirkov and S. Margenov, Eds. Cham: Springer, 2020, pp. 593–600.

[11] MFEM: Modular finite element methods library. mfem.org.

[12] REPIN, S. *A posteriori estimates for partial differential equations*, vol. 4 of *Radon Series on Computational and Applied Mathematics*. de Gruyter, Berlin, 2008.

[13] STEINBACH, O. Space-time finite element methods for parabolic problems. *Comput. Methods Appl. Math. 15*, 4 (2015), 551–566.

[14] STEINBACH, O., AND YANG, H. Space–time finite element methods for parabolic evolution equations: Discretization, a posteriori error estimation, adaptivity and solution. In *Space-Time Methods: Application to Partial Differential Equations*, U. Langer and O. Steinbach, Eds., vol. 25 of *RSCAM*. de Gruyter, Berlin, 2019, pp. 207–248.

[15] THOMÉE, V. *Galerkin finite element methods for parabolic problems*, second ed., vol. 25 of *Springer Series in Computational Mathematics*. Springer-Verlag, Berlin, 2006.

Technical Reports of the Doctoral Program

"Computational Mathematics"

2021

2021-01   J. Qi: *A tree-based algorithm on monomials in the Chow group of zero cycles in the moduli space of stable pointed curves of genus zero* Jan 2021. Eds.: S. Radu, J. Schicho

2021-02   A. Jiménez Pastor, P. Nuspl, V. Pillwein: *On C^2-finite sequences* Feb 2021. Eds.: M. Kauers, P. Paule

2021-03   A. Jiménez Pastor: *Simple differentially definable functions* Feb 2021. Eds.: M. Kauers, V. Pillwein

2021-04   U. Langer, A. Schafelner: *Simultaneous space-time finite element methods for parabolic optimal control problems* March 2021. Eds.: V. Pillwein, R. Ramlau

2021-05   U. Langer, A. Schafelner: *Space-time hexahedral finite element methods for parabolic evolution problems* March 2021. Eds.: B. Jüttler, V. Pillwein

2020

2020-01   N. Smoot: *A Single-Variable Proof of the Omega SPT Congruence Family Over Powers of 5* Feb 2020. Eds.: P. Paule, S. Radu

2020-02   A. Schafelner, P.S. Vassilevski: *Numerical Results for Adaptive (Negative Norm) Constrained First Order System Least Squares Formulations* March 2020. Eds.: U. Langer, V. Pillwein

2020-03   U. Langer, A. Schafelner: *Adaptive space-time finite element methods for non-autonomous parabolic problems with distributional sources* March 2020. Eds.: B. Jüttler, V. Pillwein

2020-04   A. Giust, B. Jüttler, A. Mantzaflaris: *Local (T)HB-spline projectors via restricted hierarchical spline fitting* March 2020. Eds.: U. Langer, V. Pillwein

2020-05   K. Banerjee, M. Ghosh Dastidar: *Hook Type Tableaux and Partition Identities* June 2020. Eds.: P. Paule, S. Radu

2020-06   A. Bostan, F. Chyzak, A. Jiménez-Pastor, P. Lairez: *The Sage Package* `comb_walks` *for Walks in the Quarter Plane* June 2020. Eds.: M. Kauers, V. Pillwein

2020-07   A. Meddah: *A stochastic multiscale mathematical model for low grade Glioma spread* June 2020. Eds.: E. Buckwar, V. Pillwein

2020-08   M. Ouafoudi: *A Mathematical Description for Taste Perception Using Stochastic Leaky Integrate-and-Fire Model* June 2020. Eds.: E. Buckwar, V. Pillwein

2020-09   A. Bostan, A. Jiménez-Pastor: *On the exponential generating function of labelled trees* July 2020. Eds.: M. Kauers, V. Pillwein

2020-10   J, Forcan, J. Qi: *How fast can Dominator win in the Maker-Breaker domination game?* July 2020. Eds.: V. Pillwein, J. Schicho

2020-11   J. Qi: *A calculus for monomials in Chow group of zero cycles in the moduli space of stable curves* Sept 2020. Eds.: P. Paule, J. Schicho

2020-12   J. Qi, J. Schicho: *Five Equivalent Ways to Describe a Phylogenetic Tree* November 2020. Eds.: M. Kauers, S. Radu

Doctoral Program

"Computational Mathematics"

Director:

Assoc. Prof. Dr. Veronika Pillwein
Research Institute for Symbolic Computation

Deputy Director:

Prof. Dr. Bert Jüttler
Institute of Applied Geometry

Address:

Johannes Kepler University Linz
Doctoral Program "Computational Mathematics"
Altenbergerstr. 69
A-4040 Linz
Austria
Tel.: ++43 732-2468-6840

E-Mail:

office@dk-compmath.jku.at

Homepage:

http://www.dk-compmath.jku.at

Submissions to the DK-Report Series are sent to two members of the Editorial Board
who communicate their decision to the Managing Editor.